LA-UR-12-25595
Approved for public release; distribution is unlimited.

Title: Developing Simplified Models of Wind Turbine Blades

Author(s): Van Buren, Kendra L.
Mollineaux, Mark G.
Hemez, Francois M.
Luscher, Darby J.

Intended for: Fiscal year 2012 report of the LDRD-DR project "intelligent wind turbines"
Report

Developing Simplified Models for Wind Turbine Blades

Kendra L. Van Buren[1]

Clemson University
Civil Engineering Department
Clemson, South Carolina

Mark G. Mollineaux[2]

Stanford University
Civil Engineering Department
Stanford, California

François M. Hemez[3]

Los Alamos National Laboratory
XTD-Division (XTD-3)
Los Alamos, New Mexico

D.J. Luscher[4]

Los Alamos National Laboratory
T-Division (T-3)
Los Alamos, New Mexico

Abstract: Simplified beam models provide a computationally efficient method for modeling the vibration of wind turbine blades. The purpose of this paper is to demonstrate the process of developing a simplified beam model of the CX-100 wind turbine blade, and quantifying its predictive capability. The motivation for this study is rooted in the development of *NLBeam*, a non-linear beam code developed at Los Alamos National Laboratory to simulate the structural dynamics response of wind turbines using the geometrically exact beam theory in a coupled atmospheric hydrodynamics solver. Verification activities used to assess the credibility of *NLBeam* are investigated. Two models of the CX-100 blade are compared: (1) a three dimensional shell model and (2) a simplified one-dimensional beam model. Two sets of experimental modal data are utilized, one with the CX-100 blade in a fixed-free condition, and one with the CX-100 blade in a fixed-free condition, with large masses applied. By exploring these different configurations of the wind turbine blade, credibility can be established regarding the ability of the FE model to predict the response to different loading conditions. Through the use of test-analysis correlation, the experimental data can be compared to model output and an assessment is given of the predictive capability of the model. *(Approved for unlimited, public release on October-xx-2012, LA-UR-12-xxxx, Unclassified.)*

---

[1] Doctoral student, Clemson University. Mailing address: Department of Civil Engineering, Clemson University, Lowry Hall, Box 340911, Clemson, SC 29634-0911. E-mail: klvan@clemson.edu.

[2] Doctoral student, Stanford University. Mailing address: Department of Civil and Environmental Engineering, 473 Via Ortega, Room 314, Mail Code 4020, Stanford University, Stanford, CA 94305. E-mail: mgm1@stanford.edu.

[3] Technical staff member, XCP-Division. Mailing address: Los Alamos National Laboratory, XCP-1, Mail Stop F644, Los Alamos, NM 87545. E-mail: hemez@lanl.gov. AIAA Senior Member.

[4] Technical staff member, T-Division. Mailing address: Los Alamos National Laboratory, T-3, Mail Stop B216, Los Alamos, NM 87545. E-mail: djl@lanl.gov.

1. Introduction

Wind power is currently being pursued in the United States to supply a major amount of installed energy. As a result, wind turbine plants are being developed at a larger scale, resulting in the production of wind turbines at an increased scale, from rotors with a diameter of 18 meters in 1985 to 120 meters in 2007[1]. Turbine-to-turbine interaction from wind turbines installed at this massive scale needs to be better understood to facilitate the expansion of wind turbine plants in an economical and efficient way, and to optimize the power output while minimizing fatigue failure. The development of modeling and simulation (M&S) techniques offers an avenue to economically study the behavior of wind turbines. However, to make such a step forward possible, understanding the state of the art in modeling wind turbine blades is extremely important.

To study wind plants in an economical way, Los Alamos National Laboratory (LANL) has developed a Computational Fluid Dynamics (CFD) wind plant software, called *WindBlade* to study the wind-to-turbine and turbine-to-turbine interactions[2]. Figure 1 illustrates a simulation of the WindBlade code applied to an idealized section of a wind plant. Integration of large-scale, high fidelity models of structural response with CFD models are often limited due to the demands on computing resources. For this reason, WindBlade currently represents the structural dynamics of the wind turbine system using rigid body dynamics for the blades and tower. The *NLBeam* finite element (FE) code, also developed at LANL, can however replace these rigid bodies, and couple realistic wind turbine elastodynamics into WindBlade without adding significant computational costs to the numerical simulation. *NLBeam* incorporates geometric nonlinearities to simulate the structural dynamic response of wind turbine blades using the geometrically exact beam theory. The incorporation of geometric nonlinearities in the implementation of *NLBeam* offers an advantage over other open-source FE formulations developed specifically to model wind turbine blades as beam elements such as FAST[3] (Fatigue, Aerodynamics, Structures, and Turbulence) and BPE[4] (Beam Property Extraction) due to the ability to account for P-Δ effects incurred from large amplitude blade deformations[5]. However, the uncertainty introduced when simplifying a high-fidelity, complex model into a low-fidelity, beam model, needs to be addressed to lend credibility to the simulation.

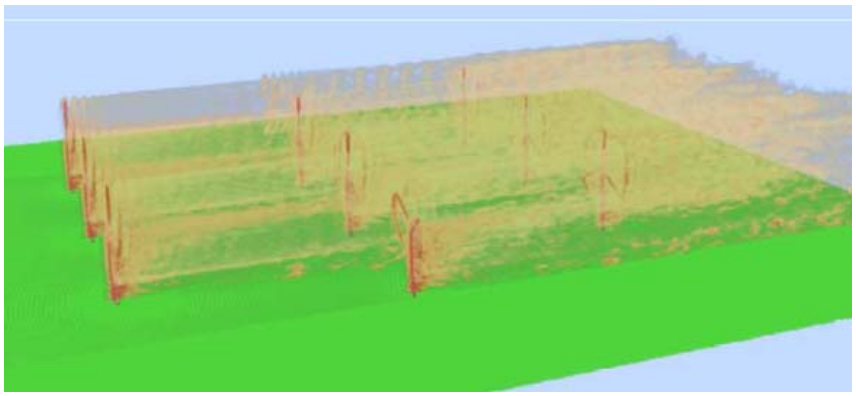

Figure 1. WindBlade model of an idealized wind farm.

This manuscript is organized as follows. First, the details of *NLBeam* are discussed in Section 2, and a brief code verification effort is provided in Section 3. The focus of the paper then turns to the development of FE models used to simulate the vibrations of the 9-meter CX-100 wind turbine blade, developed at Sandia National Laboratories. Experimental modal analysis of the CX-100 wind turbine blade, performed at the National Renewable Energy Laboratory, is discussed in Section 4. The development of the three-dimensional model is discussed in

Section 5, and of the one-dimensional beam model in Section 6. A comparison of the model predictions of the mode shapes obtained from the experimentally obtained mode shapes is provided in Section 7. The implications of the work provided herein and avenues for future study are provided in Section 8.

2. The *NLBeam* Formalism

The current availability of computing resources for engineering applications prevents the implementation of large-scale, high-fidelity models of the structural response. For this reason, *WindBlade* currently represents the structural dynamics of the wind turbine system (tower and rotor/blades) using rigid body dynamics. *NLBeam*, a FE based code developed at Los Alamos National Laboratory is being developed to couple realistic wind turbine elastodynamics into *WindBlade* without adding significant computational costs to the numerical simulation. The *NLBeam* code models wind turbine blade dynamics using the geometrically exact beam theory and is an improvement over many alternative methods because of its ability to handle geometric nonlinearities (large deformation, large strain).

In the formulation of this beam theory, sectional strains and curvatures are computed along the position of a beam accounting for local coordinate rotations. Axial and transverse shear strains are calculated by taking the derivative of the beam's position in space with respect to the undeformed distance along the beam and multiplying by a rotational matrix to calculate strains in the cross sectional direction of interest, as seen in equation (1), where Λ^T is the rotational matrix, r_n' is the position derivative, and b_1 is the direction of the cross-sectional normal:

$$\gamma_n = \Lambda^T r_n^{'} - b_1 . \tag{1}$$

The torsional rate of twist and bending curvatures are found by taking the derivative of the rotation tensor and multiplying by the rotation matrix calculating the sectional curvatures in local coordinates shown in equation (2) where Λ^T is the rotational matrix and Λ_n' is the rotation tensor:

$$\kappa_n = \Lambda^T \Lambda_n^{'} . \tag{2}$$

By substituting these values into the strain-energy equation (3) and taking the derivative in terms of both sectional strains and curvature, see equation (4), sectional forces and moments, respectively, are calculated. In equation (3), the matrix [C] represents a matrix of cross-sectional properties expanded in equation (4). For isotropic, homogeneous materials, this matrix takes a diagonal shape:

$$U = \frac{1}{2} \begin{Bmatrix} \gamma \\ \kappa \end{Bmatrix}^T [C] \begin{Bmatrix} \gamma \\ \kappa \end{Bmatrix}, \tag{3}$$

and:

$$\begin{Bmatrix} F_{Na} \\ F_{Nv2} \\ F_{Nv3} \\ F_{Mt} \\ F_{Mb2} \\ F_{Mb3} \end{Bmatrix} = \begin{bmatrix} EA_1 & & & & & \\ & GA_2 & & & 0 & \\ & & GA_3 & & & \\ & & & GJ & & \\ & 0 & & & EI_2 & \\ & & & & & EI_3 \end{bmatrix} \begin{Bmatrix} \gamma_1 \\ \gamma_2 \\ \gamma_3 \\ \kappa_1 \\ \kappa_2 \\ \kappa_3 \end{Bmatrix}. \tag{4}$$

The result of this formalism is a linear force to strain relationship in the moving beam coordinate frame. However, the relationship between generalized strains and generalized coordinates involves the rotation tensor which is inherently nonlinear.

3. Verification of the *NLBeam* Finite Element Code

Code verification can establish credibility in software codes and provide evidence of mathematical correctness in the implementation of software codes, in the absence of being able to prove that simulation models are unambiguously correct. "Spot check" code verification is performed to assure that the software is running properly, without any significant programming mistake that would negatively impact the results sought. Test beams with analytical solutions are developed in *NLBeam* to verify the ability to implement nonlinear geometric defects.

3.1 Verification of Deflection Nonlinearity and Vibration Response

A cantilever beam is developed in the *NLBeam* software to verify the nonlinear behavior and vibration response of a moment applied at the tip of the beam, as illustrated in Figure 2.

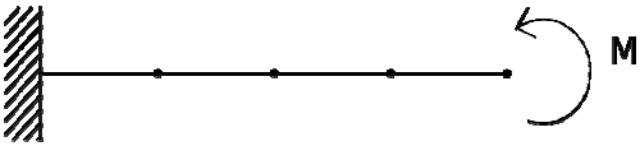

Figure 2. Illustration of the moment applied to a cantilever beam.

For the small moment application, the model follows the closed-form solution:

$$U = \frac{Mx^2}{2EI}. \tag{5}$$

where M is the applied moment, x is the x-coordinate of the beam, E is the young's modulus, and I is the area moment of inertia. This equation holds true when the small angle assumption can be applied, as shown by the agreement of *NLBeam* and the closed form solution for small moments are applied in Figure 3. However, for large moment application, nonlinear behavior becomes readily apparent due to the influence of P-Δ effects. This deviation of the tip displacement from the closed-form solution is shown in Figure 3.

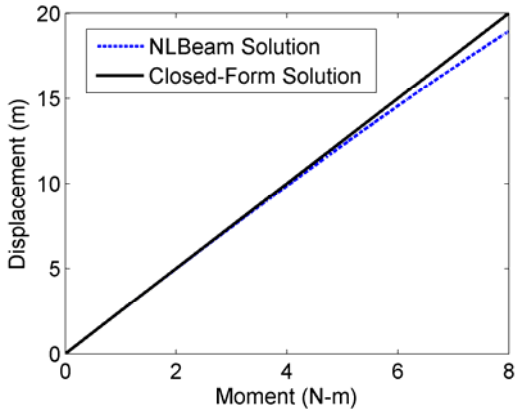

Figure 3. Deviation of the closed-form solution from *NLBeam*.

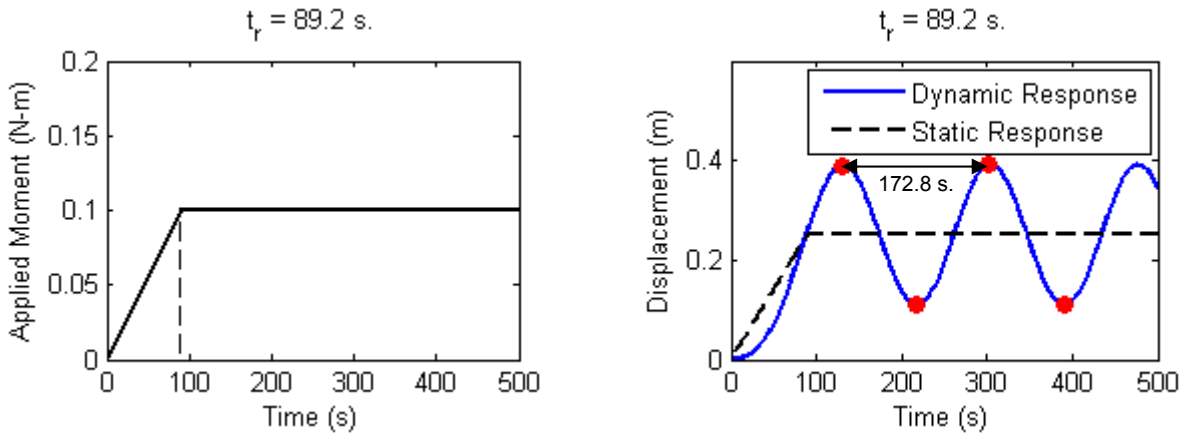

Figure 4-1. Applied load (left) and response (right) with ramped time = 89.2 sec.

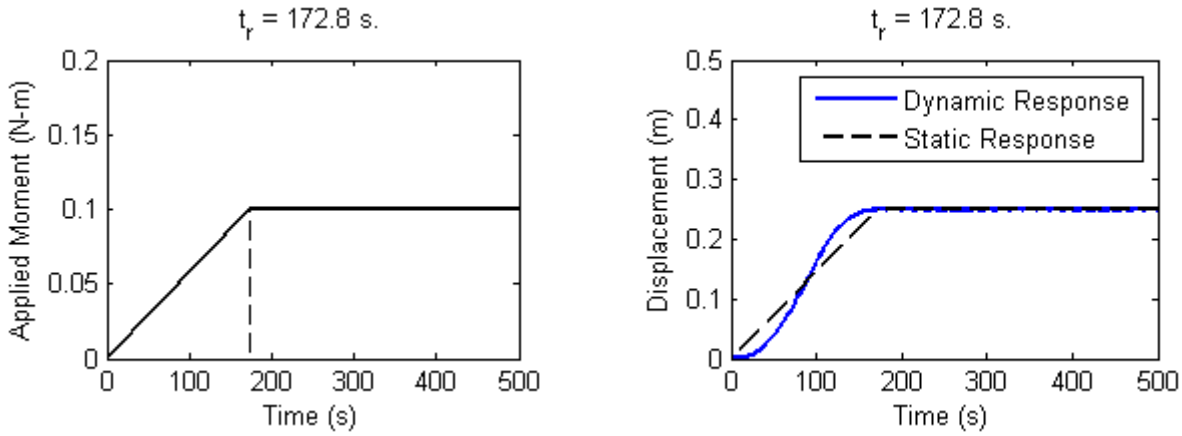

Figure 4-2. Applied load (left) and response (right) with ramped time = 172.8 sec.

The response to a ramped load is also investigated, since it is typically advantageous to use ramped loading when using a nonlinear solver. The dynamic solution of a ramped load will result in a vibration response dependent on how long the ramped load is applied to the structure, and the natural frequency of the beam. To test this behavior, a ramped load is applied to the beam as shown in the left plot of Figure 4.1, with a ramped load time of 89.2 seconds. The right plot of Figure 4.1 provides a periodic dynamic response of 172.8 seconds. Figure 4.2 shows that the amplitude of the response is significantly reduced when the ramped load applied over 172.8 seconds.

2.2 Verification of Large Angle Displacement

Stress-free rotation in a pinned beam is also evaluated by continuously applying a moment to the tip of the beam. Large angle displacement is not constrained to be solved with a linear model, which is typically performed using matrix pseudo-inversions, and becomes ill-conditioned as a result of the unconstrained nature of the set-up. The nonlinear solver, however, if able to consider drastic alterations of the geometry and not just perturbations of an initial set-up, allows for a solution. Thus, the x-displacement or y-displacement of a pinned beam should follow a sine wave when using a nonlinear solver. This test problem is illustrated in Figure 5, with the tip

displacement shown in Figure 6. Acceleration in the tip displacement of the beam is observed in Figure 6, due to a continuously applied moment at the tip of the beam.

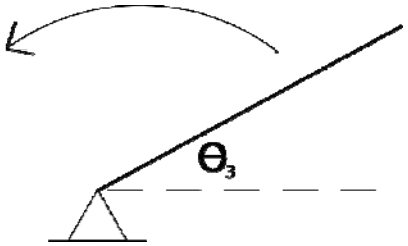

Figure 5. Illustration of the stress-free rotation of a pinned beam.

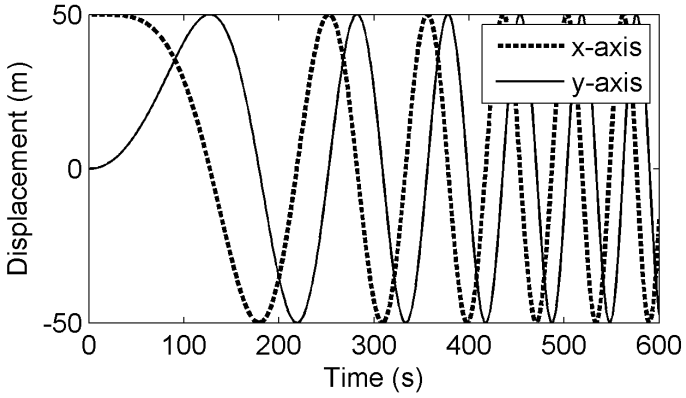

Figure 6. Tip displacement of the pinned beam.

These simple test problems do not provide a complete and exhaustive coverage of algorithmic options implemented in the software. They are, however, the minimum number of test problems needed to demonstrate a credible application of the nonlinear beam element to the *WindBlade* fluid dynamics code.

4. Experimental Modal Analysis of the Wind Turbine Blade

The focus of the paper now shifts toward the development of FE models used to simulate the vibrations of the CX-100 wind turbine blade. Two models are developed in Sections 5 and 6; a three-dimensional shell element model, and a one-dimensional beam model. Here, the details of the experimental modal data used to calibrate the models are provided.

Data obtained from experimental modal testing of the CX-100 wind turbine blade performed at the National Renewable Energy Laboratory allows the possibility of examining the predictive capability of FE models. Modal testing is performed using a roving impact hammer test of the CX-100 blade under two different set-ups: first, in a fixed-free condition, and second with an addition of two large masses. Four uni-axial accelerometers and one tri-axial accelerometer is used to collect data for hammer impacts at 65 locations: 47 in the flapwise directions, and 18 in the edgewise directions. Three test repeats were performed with a linear average and 150 Hz sampling frequency. The acceleration response is collected with 4096 sampling points in 11 seconds, and a window function is not used due to the fact that the blade response is abated. The addition a 582 kg mass and 145 kg mass at the 1.6 meter and 6.75 meter locations, respectively, is inspired by their utility in performing fatigue testing upon the blade. Figure 7 shows a photograph of this set-up, and the experimentally obtained natural frequencies are provided in Table 1.

Figure 7. CX-100 blade tested without added mass (left) and with added mass (right).

Table 1. Results of the experimental modal analysis.

Mode	Frequency (Hz) – Before Adding Weights	Frequency (Hz) – After Adding Weights	Description
1	4.35 Hertz	1.82 Hertz	1st Flap Bending
2	6.43 Hertz	2.68 Hertz	1st Lag Bending
3	11.51 Hertz	9.23 Hertz	2nd Flap Bending
4	20.54 Hertz	12.72 Hertz	3rd Flap Bending
5	23.11 Hertz	14.68 Hertz	2nd Lag Bending
6	35.33 Hertz	18.86 Hertz	4th Flap Bending

The modal data is used to calibrate the FE models developed in this study. It is desired to learn whether an equivalence exists between the loaded CX-100 blade and the unloaded blade. In particular, it will be observed if the models can accurately predict the response of the blade without further calibration after the masses are added to the simulation. Furthermore, the configuration with added masses exercises the base fixity of the blade, and has the potential to add for further insight to the boundary condition applied.

5. Development of the Three-dimensional Model

The FE model of the CX-100 wind turbine blade developed in Reference 6 using NuMAD, pre-processing software developed at Sandia National Laboratory and imported to ANSYS v. 12. This model is developed using the accurate geometry of the wind turbine blade, obtained from design specifications, and defining smeared section material properties through the use of the rule of mixtures to provide linear isotropic properties. The blade model is defined using six sections only. Figure 8 illustrates the definition of five of the six sections, together with the level of mesh discretization used in the model. A detailed discussion of the calibration can be found in Reference 7, in which the details of this process are fully developed.

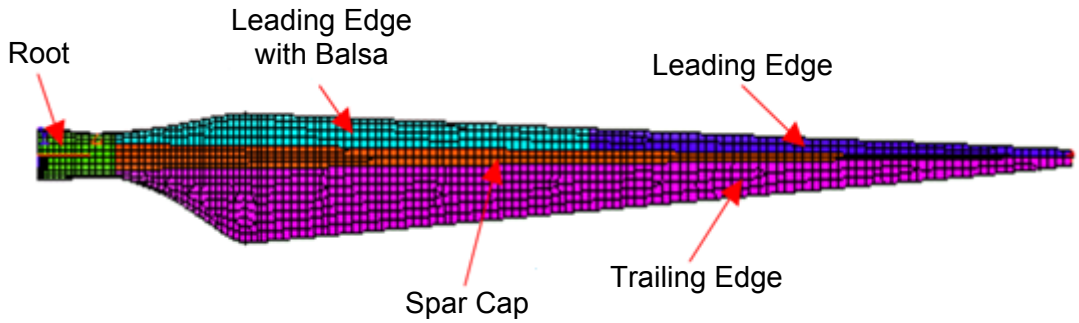

Figure 8. Definition of the CX-100 NuMAD model sections.

Measurements of the natural frequencies obtained during the NREL testing are utilized to calibrate the FE model. Instead of performing calibration as an optimization of model parameters to best-fit the experimental data, inference uncertainty quantification is performed to explore the posterior probability distribution of the statistically significant parameters. A comparison of the first three flap-wise natural frequencies to the experimentally obtained frequencies are provided in Table 2, which shows that the model is able to replicate the experimental data within 4% error.

Table 2. Experimental and simulated natural frequencies for the fixed-free model.

Mode	Description	Experimental (Hz)	Simulated (Hz)	Difference (%)
1	1st Flap	4.35 Hertz	4.26 Hertz	2.07%
3	2nd Flap	11.51 Hertz	11.45 Hertz	0.52%
4	3rd Flap	20.54 Hertz	19.85 Hertz	3.36%

To implement the masses into the simulation in an as-simplistic-as-possible manner, a central point mass is added at each cross section and then connected by springs to the nodes of the blade to adjust for the interaction between the blade and the added masses. The configuration of the springs, with the point mass in the middle, is shown in Figure 9. This modeling is adopted because exploratory FE simulations indicate that representing the masses simply as concentrated values does not adequately account for the rigidity introduced. A way to model this rigidity is through the introduction of fictitious springs. The spring constants are specified at a value of 10^8 N/m, because exploratory exercises of the springs demonstrate the natural frequencies plateau at this value, providing natural frequencies that consistently under-predict the experimental natural frequencies.

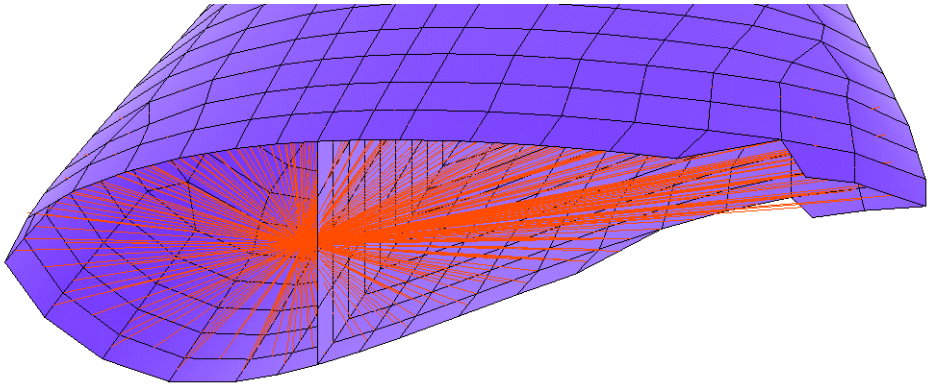

Figure 9. Illustration of the blade cross-section with added point mass and springs.

Table 3. Experimental and simulated natural frequencies for the mass-added model.

Mode	Description	Experimental (Hz)	Simulated (Hz)	Difference (%)
1	1st Flap	1.82 Hertz	1.45 Hertz	20.33%
3	2nd Flap	9.23 Hertz	8.86 Hertz	4.01%
4	3rd Flap	12.72 Hertz	11.60 Hertz	8.81%

Table 3 compares natural frequencies from the experiments to the model output. Here, the natural frequencies are consistently under-predicted by the model; however, the absolute differences for the first three modes, 0.37, 0.37, and 1.12 Hz, demonstrate an acceptable fidelity to experimental data despite the minimal calibration activities performed after the model was modified to include the added masses.

6. Development of Equivalent Simplified Beam Model

A one-dimensional model of the CX-100 is developed in ANSYS using Beam189 elements as an intermediate step, and the finalized model parameters after calibration can be transferred into *NLBeam*. Use of *NLBeam*, will account for nonlinear geometric effects, however, ANSYS is used for model development due to the use of linear experimental modal data for calibration. Beam189 elements are quadratic three-node beam elements, with six degrees of freedom at each node, thus utilizing the same inputs as required by *NLBeam* elements. The three-dimensional model, discussed in the previous section, is utilized to derive an initial set of calibration parameters for the beam model. Due to the successful test-analysis correlation of the 3-D blade model, it is assumed that the mass and stiffness distribution is accurately represented, allowing the three-dimensional model to be a defensible source to supply initial values for the beam model. The calibration parameters are the cross-sectional area, density, moment of inertia, and product of inertia. The three-dimensional FE model allows for easily obtained approximations of the material properties for use in the beam model. In this process, the beam model of the blade is discretized into equivalent 1-meter elements with an additional node placed at the 0.675 meter station to capture the effects of the tapering root section.

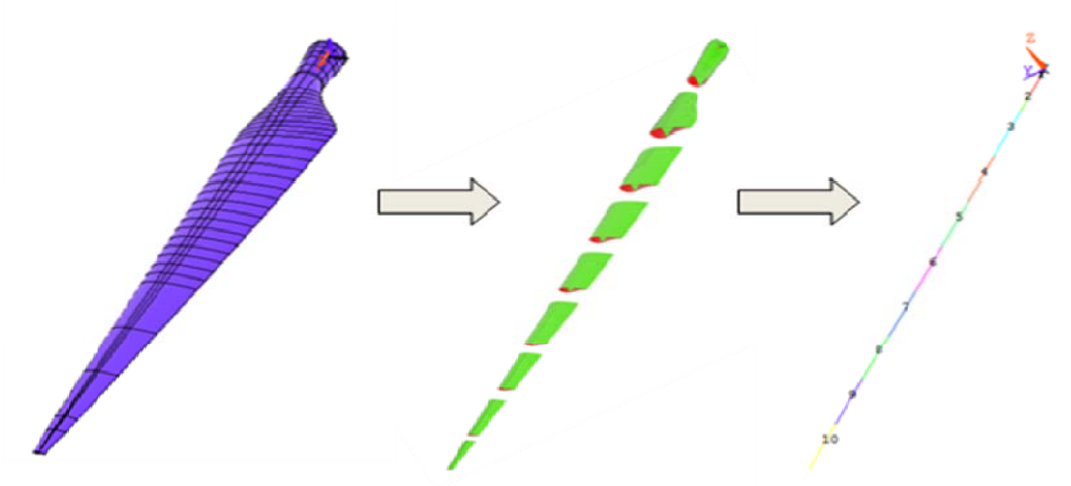

Figure 10. Deriving equivalent beam model properties of the CX-100.

The weight of the CX-100 blade is 174 kg (383 lb)[8], compared to 161 kg obtained from the calibrated 3-D FE model, resulting in a 7% error between the simulation and measurement. The

3-D model is divided into sections corresponding to the discretization of the 1-D model. These sections are used to approximate the mass distribution of the blade, and consequently, the density. The moduli of elasticity are approximated by averaging the modulus of elasticity over the length of each section.

Initial estimates of the moment of inertia are approximated by dividing the blade into sections, as shown in Figure 10, fixing the base, and applying a unit load and then back-calculating the moment of inertia from the resulting displacements, using the Young's Modulus already specified. The product of inertia, I_{xy}, assumes a value of zero for symmetric cross-sections. A genetic algorithm optimization process is used to search for the values used for the product of inertia, due to the inability to measure the product of inertia for the un-symmetric cross-sections of the blade. The moments of inertia, I_{xx} and I_{yy} and the product of inertia, I_{xy} are calibrated using the genetic algorithm because their interaction can account for the coupling between the flap-wise and edge-wise movement that occurs in the modes used to calibrate the model. To ensure that this goodness-of-fit is not a false minimum of calibration to realistic data, genetic algorithmic measures are taken to conclude that this point (a set of parameters for the simplified model) is at, or at least very near, the global optimum.

Table 4. Comparison of experimental and simulated results for the fixed-free model.

Mode	Description	Experimental (Hz)	Simulated (Hz)	Difference (%)
1	1st Flap	4.35 Hertz	4.44 Hertz	2.07%
3	2nd Flap	11.51 Hertz	11.99 Hertz	4.17%
4	3rd Flap	20.54 Hertz	20.70 Hertz	0.78%

Comparisons of the experimental and simulated natural frequencies for the simplified beam model are given in Table 4. This comparison demonstrates the ability of the genetic algorithm to calibrate the finite element model to the experimental data. Point masses are added to the beam model to determine if the mass-added natural frequencies can be accurately obtained.

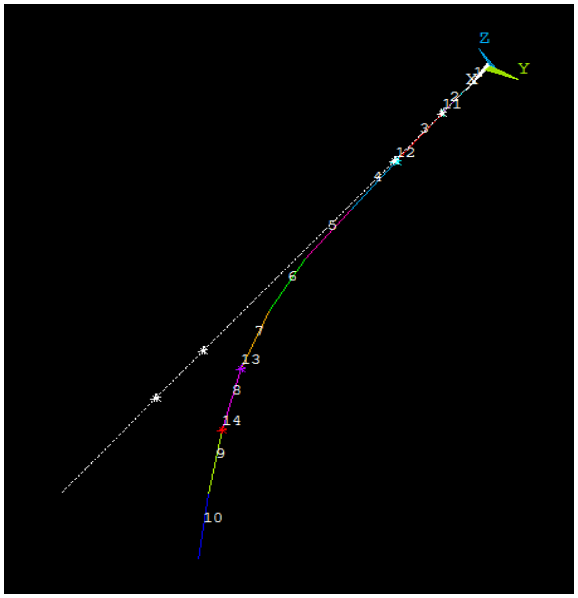

Figure 11. Illustration of 1-D beam element with added mass.

Table 5. Predictions of the modified, simplified model.

Mode	Model Results	Experimental Results	% Error
1st Flap	1.84 Hertz	1.82 Hertz	0.92%
1st Lag	2.83 Hertz	2.68 Hertz	3.44%
2nd Flap	9.41 Hertz	9.23 Hertz	4.17%
3rd Flap	12.81 Hertz	12.72 Hertz	2.20%

Table 5 provides the predictions of the natural frequencies of the mass-added configuration, compared to the experimental results. Here, the first four natural frequencies are predicted with less than 5% error. This comparison demonstrates that the simplified beam model can be used to accurately simulate overall global properties of the CX-100 wind turbine blade.

7. Comparison of Model Predictions

Thus far, the ability of the FE models to accurately replicate the natural frequencies has been discussed. However, calibration can introduce the danger of over-fitting[9]. To establish a predictive capability, the mode shapes of the simulations are compared to the experimentally obtained mode shapes. Further, the experimental data with the attached masses, is employed as a validation set.

The Modal Assurance Criterion (MAC) is a metric used to quantify the degree to which mode shapes obtained experimentally and computationally are correlated:

$$\mathrm{MAC} = \frac{\left(\Phi_{\mathrm{Test}}^{\mathrm{T}} \cdot \Phi_{\mathrm{Model}}\right)^2}{\left(\Phi_{\mathrm{Test}}^{\mathrm{T}} \cdot \Phi_{\mathrm{Test}}\right)\left(\Phi_{\mathrm{Model}}^{\mathrm{T}} \cdot \Phi_{\mathrm{Model}}\right)}, \tag{1}$$

where Φ_{Test} and Φ_{Model} are the measured and simulated mode shapes, respectively, expressed at the same degrees-of-freedom. The purpose of this analysis is to verify the extent to which the deflections are parallel for the same modes and orthogonal for different modes, providing a more complete measure of the predictive capability of the models. Figure 12 provides the mode shapes for the fixed-free experimental data, and Figure 13 provides the mode shapes for the mass-added experimental data.

The results provided in Figure 12 show the agreement of the mode shapes with experimental data. The average diagonal MAC values are 0.916 and 0.932, for the beam and three-dimensional models, respectively, and 0.430 and 0.214 for the off-diagonal terms.

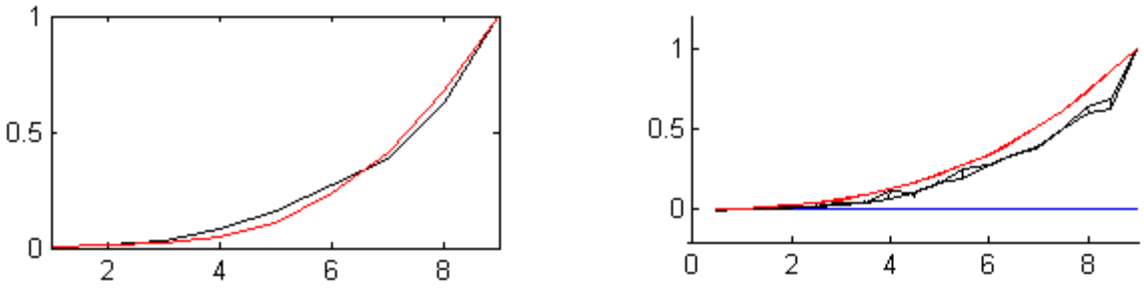

Figure 12-1. First mode shape obtained for the 1-D model (left) and 3-D model (right) for the fixed-free NREL experimental data.

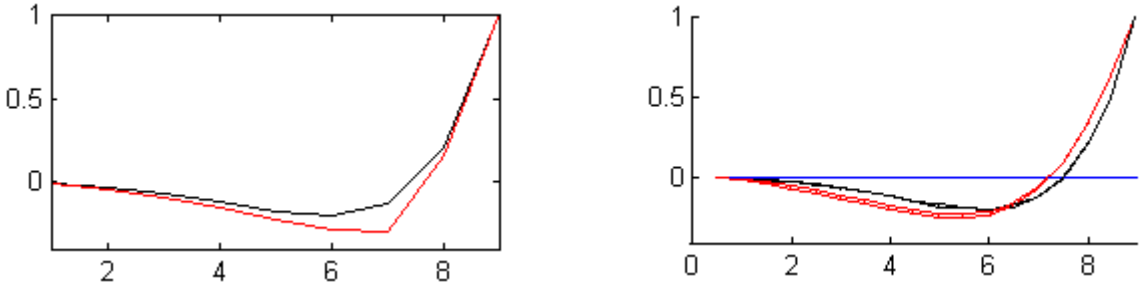

Figure 12-2. Second mode shape obtained for the 1-D model (left) and 3-D model (right) for the fixed-free NREL experimental data.

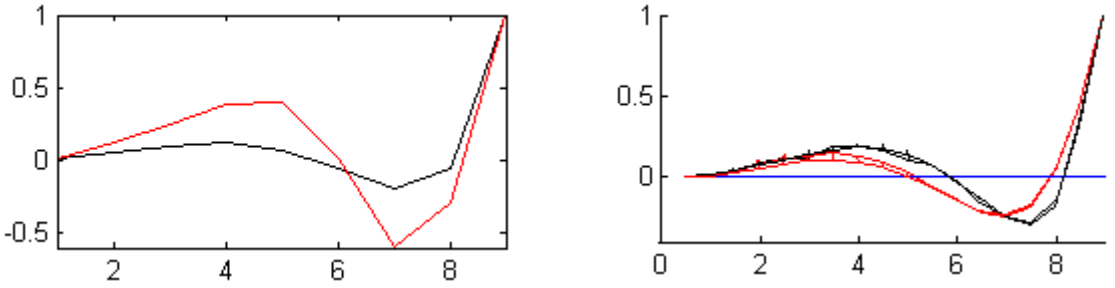

Figure 12-3. Third mode shape obtained for the 1-D model (left) and 3-D model (right) for the fixed-free NREL experimental data.

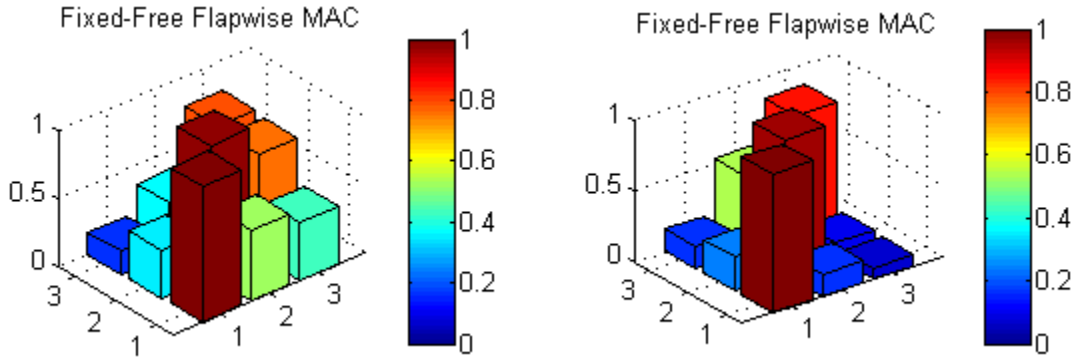

Figure 12-4. Comparison of MAC's obtained for the 1-D model (left) and 3-D model (right) for the fixed-free NREL experimental data.

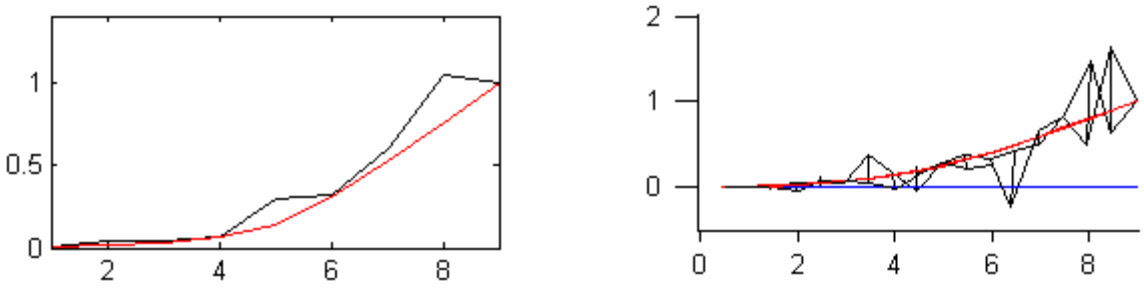

Figure 13-1. First mode shape obtained for the 1-D model (left) and 3-D model (right) for the mass-added NREL experimental data.

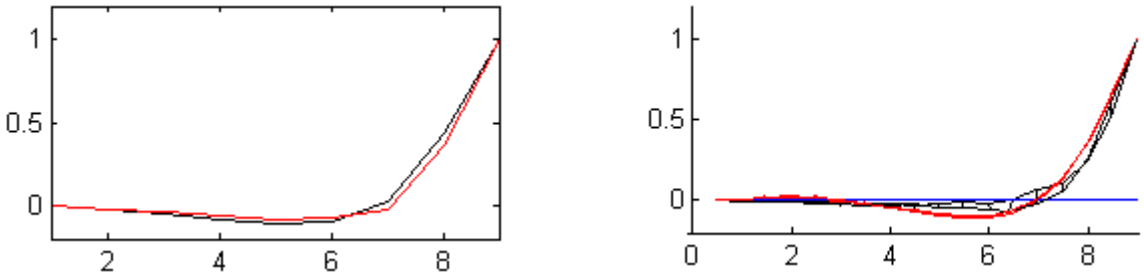

Figure 13-2. Second mode shape obtained for the 1-D model (left) and 3-D model (right) for the mass-added NREL experimental data.

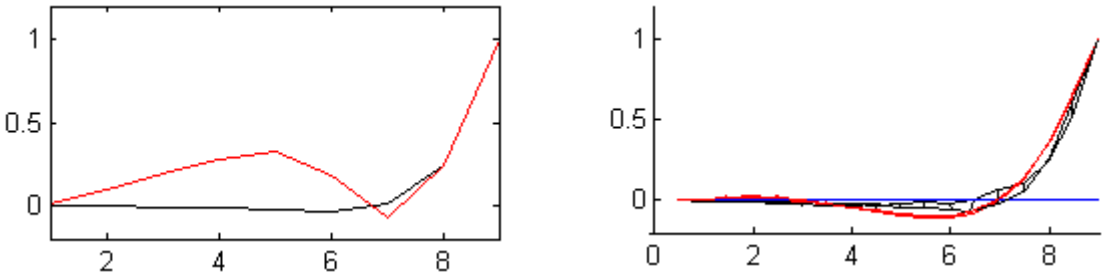

Figure 13-3. Third mode shape obtained for the 1-D model (left) and 3-D model (right) for the mass-added NREL experimental data.

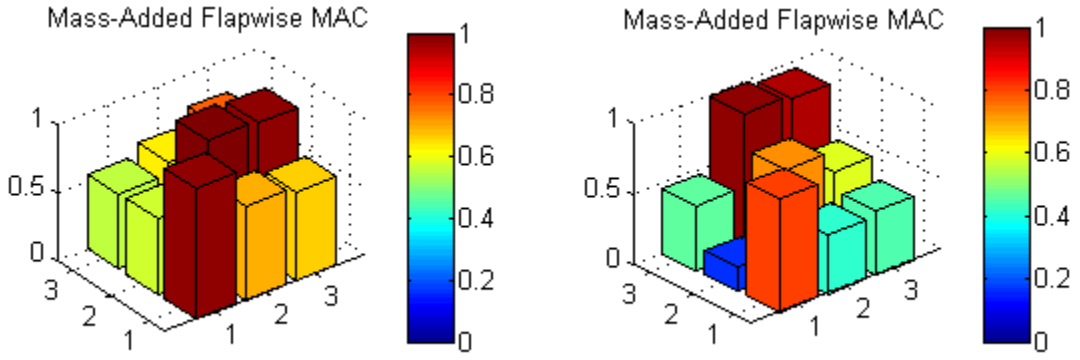

Figure 13-4. Comparison of MAC's obtained for the 1-D model (left) and 3-D model (right) for the fixed-free NREL experimental data.

The results shown Figure 13 suggest that as the boundary conditions of the finite element models are changed, the predictive capability degrades. Here, the average diagonal MAC term is 0.911 and 0.828 and off-diagonal terms are 0.842 and 0.510 for the beam model and three-dimensional models, respectively. The high off-diagonal terms can be attributed to modal aliasing, which is especially applicable to the beam model due to the use of only nine nodes to define the mode shape. This comparison also demonstrates that the beam model provides a more accurate prediction of the mode shape vectors than the three-dimensional model. This is a promising result that can be used to justify the use of beam elements.

The addition of the masses to the simulation provides a stark change in the boundary conditions. Thus, the authors view this test analysis correlation as providing a more realistic limitation of the finite element model, due to the limited calibration exercises employed to reach the model predictions.

8. Conclusion

This manuscript takes a step towards understanding the practical limitations of using a simplified beam model to simulate the vibrations of wind turbine blades. First, the formulation of the nonlinear FE solver developed at Los Alamos National Laboratory, *NLBeam*, is provided. Code verification activities are discussed to demonstrate that the software is properly implemented and ready for use. Two FE models of varying complexity are also developed to simulate the CX-100 wind turbine blade. Experimental modal data collected from testing performed at the National Renewable Energy Laboratory is used to assess the accuracy of the simulation output. The two models are both capable of replicating the fixed-free experimental data within 5% accuracy. The agreement degrades for the mass-added experimental data, however, with an error of 20% for the first mode of the three-dimensional model.

The results provided herein demonstrate that the simplified beam models are capable of replicating vastly different experimental configurations. However, it is emphasized that the experimental data only provides representation of reality that is limited to the linear behavior of the wind turbine blade. Wind turbine blades will typically undergo loading that exercise nonlinear behavior. The appropriateness of modal data to calibrate beam models of wind turbine blades will be investigated in future studies. Further, the response of wind turbines modeled with *NLBeam*, and coupling *NLBeam* with an atmospheric hydrodynamics solver to study wind turbines at the plant scale will be pursued. Robust optimal metrics will also be applied as a surrogate to quantify model form effects on model predictions, lending further credibility to model predictions.

9. Acknowledgements

This work is performed under the auspices of the Laboratory Directed Research and Development project "Intelligent Wind Turbines" at Los Alamos National Laboratory (LANL). The authors are grateful to Curtt Ammerman, project leader, for his support. LANL is operated by the Los Alamos National Security, LLC for the National Nuclear Security Administration of the U.S. Department of Energy under contract DE-AC52-06NA25396.

Bibliographical References

[1] Ashwill, T., "Materials and innovations for large blade structures: research opportunities in wind energy technology," *50th AIAA Structures, Structural Dynamics, and Materials Conference*, 2009.

[2] U.S. Department of Energy, "HIGRAD/Windblade wind generation modeling and simulation," 2010.

[3] Jonkman, J.M., Buhl Jr., M.L., "FAST user's guide," *Report NREL/EL-500-29798*, National Renewable Energy Laboratory, Golden, Colorado, 2005.

[4] Malcolm, D.J., Laird, D.L., "Extraction of equivalent beam properties from blade models," *Wind Energy*, Vol. 10, No. 2, pp. 135-157, 2007.

[5] Dalton, S., Monahan, L., Stevenson, I, Luscher, D.J., Park, G., Farinholt, K, "Experimental assessment of *NLBeam* for modeling large deformation structural dynamics," *30th International Modal Analysis Conference*, Jacksonville, Florida, Jan. 30-Feb. 2, 2012.

[6] Mollineaux, M., Van Buren, K., Hemez, F.M., "Simulating the dynamics of wind turbine blades: Part I, model development and verification," *13th AIAA Non-deterministic Approaches Conference*, Denver, Colorado, April 4-7, 2010.

[7] Van Buren, K., Mollineaux, M., Hemez, F.M., "Simulating the dynamics of wind turbine blades: Part II, uncertainty quantification and model validation," *13th AIAA Non-deterministic Approaches Conference*, Denver, Colorado, April 4-7, 2010.

[8] Paquette, J., van Dam, J., Hughes, S., "Structural testing of 9-m carbon fiber wind turbine research blades," *AIAA Wind Energy Symposium*, Reno, Nevada, 2007. (Also, NREL Report NREL/CP-500-40985.)

[9] Hemez, F.M., Ben-Haim, Y., "The good, the bad, and the ugly of predictive science," *4th International Conference on Sensitivity Analysis of Model Output*, Santa Fe, New Mexico, March 2004.

(This technical report contains 17 pages.)